Bremsstrahlung in intermediate-energy electron scattering by a La atom

A. V. Korol'

Russian Marine Technical University, 198262 St. Petersburg, Russia

A. G. Lyalin and A. S. Shulakov

Research Physics Institute at the St. Petersburg State University, 198904 St. Petersburg, Russia

A. V. Solov'ev

A. F. Ioffe Physicotechnical Institute, Russian Academy of Sciences, 194021 St. Petersburg, Russia
(Submitted 9 June 1995)
Zh. Éksp. Teor. Fiz. **109**, 1174–1187 (April 1996)

We calculate the cross section and angular distribution of polarization bremsstrahlung in 0.2–10 keV electron scattering by a La atom near the $4d$-subshell ionization potential, $\omega=100$–200 eV. We suggest a simple semiempirical method for calculating the polarization bremsstrahlung spectra. © *1996 American Institute of Physics.* [S1063-7761(96)00704-4]

1. INTRODUCTION

Below we give the results of our calculations of the cross section and angular distribution of bremsstrahlung produced in the scattering of intermediate-energy electrons (0.2–10 keV) by a La atom in the ground state.

Two different mechanisms are responsible for bremsstrahlung in electron–atom collisions. The first is known as "ordinary" bremsstrahlung, which occurs as a result of the braking of a charged particle by the static field of an atom.[1] For more than 80 years, starting with the discovery of x rays by Roentgen, this was thought to be the only process responsible for the formation of bremsstrahlung. The second mechanism is known as polarization, or "atomic," bremsstrahlung, and operates because of dynamic polarization of the atom by an incident particle.[2]

The polarization mechanism leads to broad maxima in the emission spectra near the ionization potentials of atomic multielectron shells. The existence of such maxima was predicted by theory[3] and discovered experimentally for xenon,[5] La, and the lanthanides.[5,6] Practically all the radiation at these maxima is formed by the polarization mechanism.

Calculations of bremsstrahlung spectra that allow for the polarization mechanism were carried out earlier for Ar, Xe, and La atoms in the nonrelativistic Born approximation[4,7,8] and for Xe and Ba in the partial-wave approximation.[9,10]

Polarization bremsstrahlung is even more important in ion–atom and atom–atom collisions, since in such cases ordinary bremsstrahlung is strongly suppressed due to the large masses of the colliding particles. Polarization bremsstrahlung spectra formed in the collisions of heavy nonrelativistic particles were calculated in Refs. 11–14.

Typically, when calculating polarization bremsstrahlung spectra, one must take into account multielectron correlations. To this end, Amus'ya *et al.*[7] and Avdonina *et al.*[8] used the method of random phase approximation with exchange (RPAE). This method, however, incorporates only a fraction of the correlation effects and provides a poor description of the experimental data on the photoabsorption of La (see Ref. 15). The theoretical results can be improved considerably by

employing the method of the generalized random phase approximation with exchange (GRPAE), which allows for the multielectron corrections related to the transformation of the atomic core.[15–18]

In this paper we suggest a simple approximate method for calculating the cross section of polarization bremsstrahlung near the ionization potentials of atomic multielectron shells. The main advantage of the method rests in the possibility of extracting information about the atomic dynamic structure directly from the experimental data on photoabsorption, which makes it possible to avoid complicated numerical calculations that allow for multielectron correlations. The simplicity of the method also makes it possible to calculate the polarization bremsstrahlung cross section for more complex systems, such as molecules, clusters, and solids.

We give the results of calculations of the spectral and angular distributions of bremsstrahlung photons done with different approximation schemes, and also the dependence of the cross section and angular distribution of bremsstrahlung on the incident electron energy.

2. THE BORN APPROXIMATION AND THE PERTURBED PARTIAL-WAVE APPROXIMATION; CORRELATION EFFECTS

In the dipole approximation the amplitudes of ordinary and polarization bremsstrahlung are

$$f^{\text{ord}}=\langle \mathbf{p}_2|\mathbf{e}\cdot\mathbf{d}|\mathbf{p}_1\rangle,$$

$$f^{\text{pol}}=\sum_n \left(\frac{\langle \mathbf{p}_2 n|V_c|\mathbf{p}_1 0\rangle\langle 0|\mathbf{e}\cdot\mathbf{D}(\omega)|n\rangle}{\omega_{0n}+\omega+i\delta} \right.$$
$$\left. +\frac{\langle n|\mathbf{e}\cdot\mathbf{D}(\omega)|0\rangle\langle \mathbf{p}_2 0|V_c|\mathbf{p}_1 n\rangle}{\omega_{0n}-\omega} \right). \tag{1}$$

Here **e** is photon polarization vector, $\mathbf{e}\cdot\mathbf{d} = \mathbf{e}\cdot\mathbf{r}$ is the dipole interaction operator, $\mathbf{e}\cdot\mathbf{D}(\omega)$ is the operator of the effective dipole interaction of an atomic electron with the electromagnetic field, V_c is the Coulomb interaction operator, $\omega_{0n}=E_0-E_n$ is the difference in energies of the ground ($|0\rangle$) and excited ($|n\rangle$) states of the atom, ω is the photon
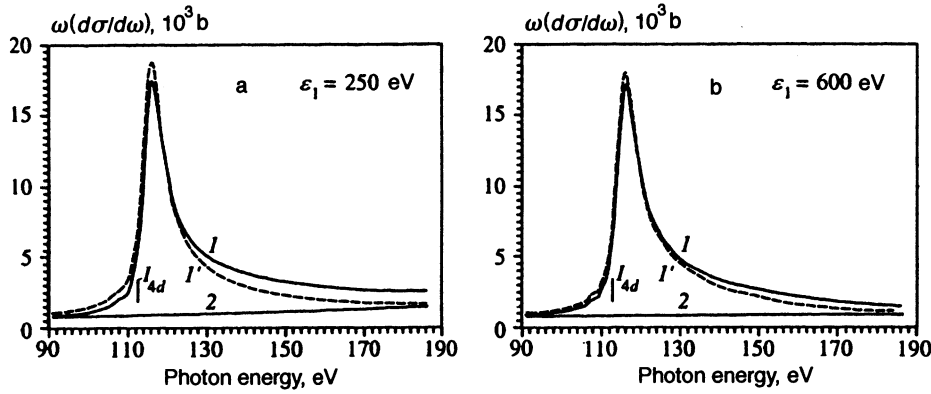
FIG. 1. Total bremsstrahlung cross section (curves *1*), the bremsstrahlung cross section without interference, i.e., the sum of ordinary and polarization bremsstrahlung (curves *1'*), and the ordinary bremsstrahlung cross section (curves *2*).

energy, and $|p_{1,2}\rangle$ are the wave functions of the incident and scattered electrons. The sum over n combines summation over the discrete excitation spectrum and integration over the continuous excitation spectrum.

When calculating the matrix elements of the operator $e \cdot D(\omega)$ we use both the one-electron Hartree–Fock approximation (here $D(\omega) = d$) and the multielectron RPAE method.[19] The effect of the transformation of the atomic core on the polarization bremsstrahlung amplitude can be taken into account by using in (1) the wave functions of excited states calculated with the Hartree–Fock field of an ion with one vacancy. Such a choice of wave functions together with the use of the experimental data on the ionization potentials in the RPAE method constitutes the basis of GRPAE (Ref. 15).

The bremsstrahlung differential cross section is given by the following expression (here we use the atomic system of units):[20]

$$\omega \frac{d\sigma}{d\omega} = \frac{1}{(2\pi)^4} \frac{\omega^4}{c^3} \frac{p_2}{p_1} \int d\Omega_{p_2} \int d\Omega_\gamma \sum_\lambda |f_{BrS}|^2, \quad (2)$$

where c is the speed of light, $p_{1,2}$ are the momenta of the incident and scattered electrons, $d\Omega_{p_2}$ and $d\Omega_\gamma$ are solid angle elements for the scattered electron and emitted photon, λ is the photon polarization, and f_{BrS} is total bremsstrahlung amplitude, which combines the amplitude of ordinary bremsstrahlung, f^{ord}, and that of polarization bremsstrahlung, f^{pol}.

The expression for the cross section of bremsstrahlung emitted by intermediate-energy electrons can be obtained by substituting (1) into (2). By expanding the wave function of the incident particle in partial waves (the DPWA method) we can write the bremsstrahlung differential cross section as an infinite sum of partial cross sections each of which contains three terms, with two terms corresponding to ordinary and polarization bremsstrahlung and the third corresponding to their interference:

$$\omega\left(\frac{d\sigma}{d\omega}\right)_{PW} = \sum_{l=0}^{\infty} \omega\left(\frac{d\sigma}{d\omega}\right)_l$$

$$= \omega\left(\frac{d\sigma}{d\omega}\right)_{PW}^{ord} + \omega\left(\frac{d\sigma}{d\omega}\right)_{PW}^{pol} + \omega\left(\frac{d\sigma}{d\omega}\right)_{PW}^{int}. \quad (3)$$

Here l is the orbital angular momentum of the incident electron. Analytical expressions for the terms in (3) are given in Ref. 21.

As the incident-electron energy increases, the convergence of the series (3) worsens. Hence in calculations we employed the following procedure: we found the first 31 partial cross sections numerically by using the FORTRAN-77 version of the program described in Ref. 22. The remainder of the sum was calculated analytically by the method suggested in Ref. 23.

Curves *1* and *2* in Fig. 1a illustrate the spectral distribution of the total and ordinary bremsstrahlung for an electron with an energy $\varepsilon_1 = 250$ eV calculated by GRPAE. The calculation was carried out using the experimental value of the $4d$-subshell ionization potential $I_{4d} = 113.2$ eV (Ref. 24). Figure 1a shows that the spectrum has a maximum above the $4d$-subshell ionization potential for the La atom. At peak value ($\omega_{max}^{GRPAE} = 116.4$ eV) the polarization bremsstrahlung cross section is almost 20 times greater than the ordinary bremsstrahlung cross section. For $\omega > \omega_{max}$ the cross section diminishes as the emitted-photon energy grows, but far above the $4d$-threshold the cross section remains higher than below it. Such behavior of the bremsstrahlung cross section is caused by descreening of the $4d$-subshell.[25,26] Physically descreening can be explained by the fact that for frequencies $\omega \gg I_{4d}$ the $4d$-subshell electrons may be considered free and, hence, have no dipole moment. Such electrons do not emit radiation in the dipole mode and contribute nothing to the screening of the atomic nucleus. Consequently, an incident electron emits radiation in the field of an ion with a charge $Z - N_{out}$, where Z is the charge of the nucleus, and N_{out} is the number of outer atomic electrons with an ionization potential $I_{out} \ll \omega$. Formally, descreening occurs because of destructive interference between ordinary and polarization bremsstrahlung. In Fig. 1a this is illustrated by the dashed curve *1'*, which depicts the total contribution of the ordinary and polarization bremsstrahlung cross sections without allowance for the interference term in (3):

$$\omega\left(\frac{d\sigma}{d\omega}\right)_{PW}' = \omega\left(\frac{d\sigma}{d\omega}\right)_{PW}^{ord} + \omega\left(\frac{d\sigma}{d\omega}\right)_{PW}^{pol}.$$

We see that at photon frequencies $\omega \gg I_{4d}$ the polarization bremsstrahlung cross section is negligible compared to
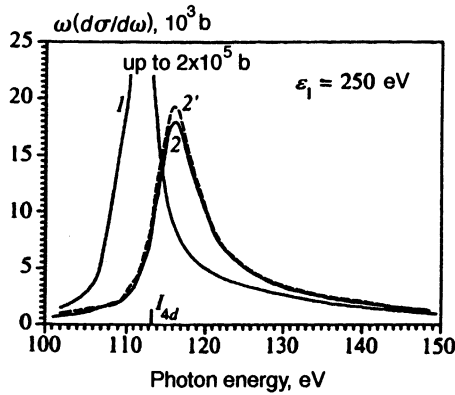
FIG. 2. Polarization bremsstrahlung cross section calculated in different approximations: curve *1* depicts the results obtained by the Hartree–Fock method within the partial-wave formalism, curve *2* depicts the results obtained by GRPAE within the partial-wave formalism, and curve *2'* depicts the results obtained by GRPAE within the Born approximation.

the ordinary bremsstrahlung cross section, in contrast to the total bremsstrahlung cross section. Hence a meaningful description of the bremsstrahlung spectrum at high frequencies requires taking into account the interference term.

At the same time, as the incident-electron energy ε_1 grows, the relative contribution of interference to the total bremsstrahlung cross section $\omega(d\sigma/d\omega)_{\mathrm{PW}}$ drops. The point is that the polarization bremsstrahlung cross section is formed at distances $r \sim q_{\min}^{-1}$ (Refs. 7 and 27). Here $q_{\min} = p_1 - p_2$ is the minimum momentum transfer, which can be estimated from the approximate relationship $q_{\min} \approx \omega/p_1$, valid provided that the photon energy is low compared to the incident-electron energy, $\omega \ll \varepsilon_1$. For distances $r \sim p_1/\omega \gg R_{\mathrm{at}}$ we have the corresponding orbital angular momentum $l_{\mathrm{eff}}^{\mathrm{pol}} \sim r p_1 = p_1^2/\omega \equiv 2\varepsilon_1/\omega$, which increases linearly with ε_1. Here R_{at} is the size of the atom.

On the other hand, the ordinary bremsstrahlung cross section is formed at distances $r \leq R_{\mathrm{at}}$, with the result that $l_{\mathrm{eff}}^{\mathrm{ord}} \sim p_1 R_{\mathrm{at}}$ increases in proportion to $p_1 = \sqrt{2\varepsilon_1}$. Hence as ε_1 grows, the partial amplitudes of the ordinary and polarization bremsstrahlung become finite at essentially different values of angular momenta, $l^{\mathrm{ord}} \ll l^{\mathrm{pol}}$, which leads to a small contribution of the interference term in (3).

Curves *1*, *1'*, and *2* in Fig. 1b illustrate, respectively, the ω-dependence of $\omega(d\sigma/\delta\omega)_{\mathrm{PW}}$, $\omega(\delta\sigma/d\omega)'_{\mathrm{PW}}$, and $\omega(d\sigma/d\omega)_{\mathrm{PW}}^{\mathrm{ord}}$ for an incident electron with an energy $\varepsilon_1 = 600$ eV. In this case the agreement between $\omega(d\sigma/\delta\omega)_{\mathrm{PW}}$ and $\omega(d\sigma/d\omega)'_{\mathrm{PW}}$ is much better, which illustrates the reduction of the contribution of interference as the energy of the incident electron grows.

Near the peak, correlations have a stronger effect on the magnitude of the bremsstrahlung cross section than interference. GRPAE allows for most of the correlations. Curves *1* and *2* in Fig. 2 depict the dependence on the photon energy of the polarization component of the bremsstrahlung spectrum $\omega(d\sigma/d\omega)_{\mathrm{PW}}^{\mathrm{pol}}$ calculated in the Hartree–Fock approximation and by GRPAE, respectively. Both calculations use the experimental value of the $4d$-subshell ionization potential. Both curves were obtained within the partial-wave formalism. The electron energy was 250 eV.

Figure 2 shows that allowing for multielectron corrections in GRPAE lowers the value of the bremsstrahlung cross section by a factor greater than 20 and moves the peak by 4 eV toward higher energies. This drastic discrepancy between the results obtained in the Hartree–Fock approximation (and the closely related RPEA method) and in GRPAE may arise because in the latter method one allows for the transformation of the atomic core. This transformation leads to a screening of the Coulomb field of the hole acting on the electron in excited states and, therefore, to a decrease in the bremsstrahlung cross section.

Screening is essential only when the characteristic excitation time is longer than the time it takes the atomic shells to transform in the field of the hole.[15] This leads to a decrease in the polarization bremsstrahlung cross section near the threshold, since here the excitation time exceeds the relaxation time. Far from the threshold the opposite is true, so that relaxation ceases to play any role. As a result the maximum at the threshold shifts toward higher energies.

Note that calculating the polarization bremsstrahlung cross section within the partial-wave formalism and at the same allowing for corrections introduced by GRPAE constitutes an extremely complicated problem. Below we describe a semiempirical method that allows for a simple and yet fairly precise calculation of the polarization bremsstrahlung cross section without using directly this laborious process.

First, the dependence of the polarization part of the spectrum on the way in which the wave functions of the scattered particle are chosen is weaker than for ordinary bremsstrahlung. The explanation is that, as noted earlier, polarization bremsstrahlung is formed primarily at large distances, where the atomic field is weak. Consequently, even with intermediate-energy incident electrons[21] polarization bremsstrahlung can be studied in the first Born approximation:[3]

$$\omega\left(\frac{d\sigma}{d\omega}\right)_{\mathrm{B}}^{\mathrm{pol}} = \frac{16}{3}\frac{\omega^4}{c^3 p_1^2} \int_{p_1-p_2}^{p_1+p_2} \frac{dq}{q}|\alpha(\omega,q)|^2. \tag{4}$$

Here $q = |\mathbf{p}_1 - \mathbf{p}_2|$ is the momentum transferred to the atom, and $\alpha(\omega,q)$ is the generalized atomic polarizability, which becomes the ordinary dynamic polarizability in the limit of small values of q.

The curve *2'* in Fig. 2 represents the spectrum (4), with the generalized $4d$-subshell polarizability $\alpha_{4d}(\omega,q)$ calculated in GRPAE. Clearly, with a 10% accuracy (in the vicinity of the peak) the Born curve reproduces the results of calculations in the partial-wave approximation (curve 2) even for an incident electron with an energy $\varepsilon_1 = 250$ eV. As ε_1 increases, the agreement between the Born calculation and the partial-wave formalism noticeably improves. Hence the polarization part of bremsstrahlung depends to a greater extent on allowing for the correlation corrections to the excited-state wave functions and to the dipole-interaction than on the choice of the wave functions of the scattered particle.

3. A SEMIEMPIRICAL METHOD FOR CALCULATING POLARIZATION BREMSSTRAHLUNG

To allow for the effect of correlations on polarization bremsstrahlung the following approach can be taken.[10,28] We write the generalized polarizability $\alpha(\omega,q)$ as

$$\alpha(\omega,q) = \alpha(\omega)G(\omega,q), \tag{5}$$

where $\alpha(\omega)$ is the dynamic polarizability. As a result the expression (4) for the polarization bremsstrahlung cross section is modified:

$$\omega\left(\frac{d\sigma}{d\omega}\right)_B^{pol} = \frac{16}{3}\frac{\omega^4}{c^3 p_1^2}|\alpha(\omega)|^2 \int_{p_1-p_2}^{p_1+p_2}\frac{dq}{q}|G(\omega,q)|^2. \tag{6}$$

Our assumption is that the factor $\alpha(\omega)$ contains all the information about the atomic correlations, while the function $G(\omega,q)$ is weakly sensitive to correlations and, hence, can be calculated in the Hartree–Fock approximation.

On the basis of the above assumption we introduce the following approximate representation for $\alpha(\omega,q)$:

$$\alpha(\omega,q) \approx \alpha^{exact}(\omega)\frac{\alpha^{HF}(\omega,q)}{\alpha^{HF}(\omega)}$$

$$\equiv \alpha^{exact}(\omega)\cdot G^{HF}(\omega,q), \tag{7}$$

where $\alpha^{exact}(\omega)$ is the "exact" atomic dynamic polarizability, and $G^{HF}(\omega,q)$ is the ratio of the generalized atomic polarizability to the ordinary atomic polarizability, both calculated in the Hartree–Fock approximation.

The imaginary part of the dipole polarizability is related to the photoabsorption cross section $\omega_\gamma(\omega)$ by the optical theorem

$$\text{Im }\alpha^{exact}(\omega) = \frac{c}{4\pi\omega}\sigma_\gamma(\omega), \tag{8}$$

while the real part of the polarizability, $\text{Re }\alpha^{exact}(\omega)$, can be calculated via the dispersion relation

$$\text{Re }\alpha^{exact}(\omega) = \frac{c}{2\pi^2}\int_0^\infty d\omega'\frac{\sigma_\gamma(\omega')}{\omega'^2 - \omega^2}. \tag{9}$$

By using the experimental values of $\sigma_\gamma(\omega)$ we can restore the "exact" dynamic polarizability $\alpha^{exact}(\omega)$, which allows for all the correlation corrections.

Curves 1 and 2 in Fig. 3 illustrate the frequency dependence of the dipole polarizability $\alpha(\omega)$ calculated, respectively, in the Hartree–Fock approximation and in GRPAE. The curves 3 represent the "exact" polarizability $\alpha^{exact}(\omega)$ found from the experimental data on photoabsorption[4,29,30] and the relationships (8) and (9). The integration in (9) is done in the photon frequency range from 0.01 to 30 keV, which provides the main contribution to $\text{Re }\alpha^{exact}(\omega)$.

The polarizability calculated by the second method is in better agreement with $\alpha^{exact}(\omega)$ than the polarizability α^{HF} calculated in the one-electron Hartree–Fock approximation. The reason why α^{GRPAE} differs from $\alpha^{exact}(\omega)$ is that GRPAE considers only a fraction of the multielectron correlations. An additional difference may be introduced by errors in the experimental values of $\sigma_\gamma(\omega)$.
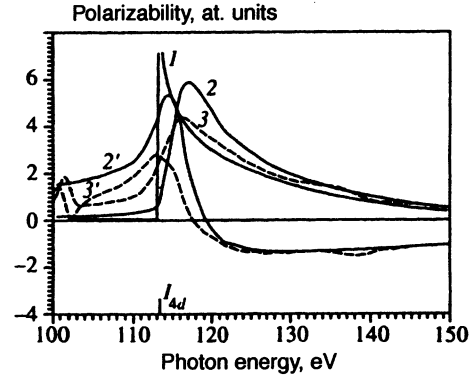

FIG. 3. The real (curves $2'$ and $3'$) and the imaginary (curves 1, 2, and 3) parts of the atomic polarizability calculated in different approximations: curve 1 corresponds to the Hartree–Fock approximation, curves 2 corresponds to GRPAE, and curves 3 are obtained from the dispersion relation and the experimental photoabsorption spectrum.

Now let us see how $G(\omega,q)$ depends on correlations. We immediately note that for photon frequencies that are much higher than the $4d$-subshell ionization potential, $\omega \gg I_{4d}$, the function $G(\omega,q)$ does not depend on correlation corrections. Indeed, here the generalized polarizability $\alpha_{4d}(\omega,q)$ is expressed in terms of the form factors of the $4d$-subshell, $\alpha_{4d}(\omega,q) = -F_{4d}(q)/\omega^2$, so that $G_{4d}^{\omega \gg I_{4d}} = F_{4d}(q)/N_{4d}$, where $N_{4d} = 10$ is the number of $4d$-electrons, is correlation-independent.

At $\omega \sim I_{4d}$ the function $G(\omega,q)$ has no simple analytical expression; hence the dependence of G on the correlation corrections was analyzed numerically. Curves 1 and 2 in Fig. 4 illustrate the dependence of the square of the absolute value ($|G^{HF}(\omega,q)|^2$) of the function calculated in the Hartree–Fock approximation on the momentum transfer q for photon energies $\omega_1 = \omega_{max}^{pol} = 116.2$ eV and $\omega_2 = 140$ eV. The dashed curves $1'$ and $2'$ represent a similar dependence for $|G^{GRPAE}(\omega,q)|^2$.

We see that for $|G(\omega,q)|^2$ a one-electron Hartree–Fock calculation and a GRPAE calculation produce very similar results. The good agreement between the functions
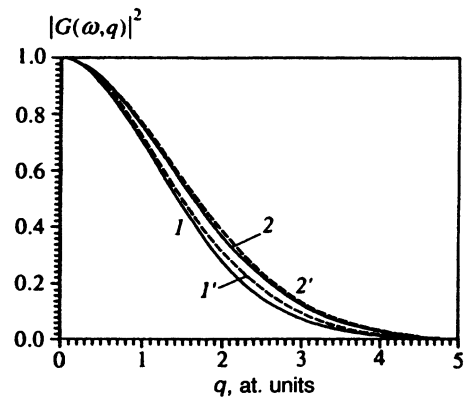

FIG. 4. $|G(\omega,q)|^2$ calculated in the Hartree–Fock approximation (curves 1 and 2) and in GRPAE (curves $1'$ and $2'$) for different frequencies: 1—$\omega = 116.2$ eV, and 2—$\omega = 140$ eV.
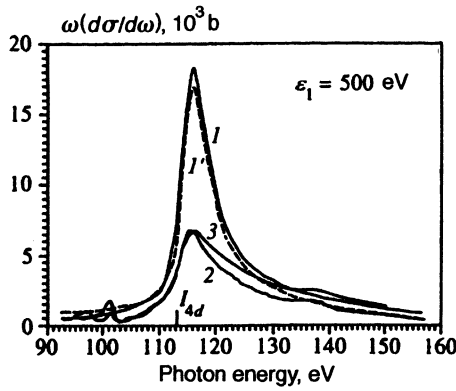
FIG. 5. Comparing the polarization bremsstrahlung cross sections calculated in the new approximation and in GRPAE: curve 1 corresponds to $\alpha^{GRPAE}(\omega)$ and $G^{HF}(\omega,q)$, curve $1'$ corresponds to $\alpha^{GRPAE}(\omega)$ and $G^{GRPAE}(\omega,q)$, curve 2 corresponds to the polarizability obtained from the dispersion relation and $G^{HF}(\omega,q)$, and curve 3 represents the experimental data of Zimkina et al.[31]

FIG. 6. The polarization bremsstrahlung cross section vs the incident-electron energy for different approximations: curve 1 corresponds to GRPAE and the Born approximation, curve 2 corresponds to GRPAE in the partial-wave formalism, curve $2'$ represents the sum of the first 31 partial cross sections, curve 3 corresponds to polarization bremsstrahlung in the new approximation, curve 4 corresponds to ordinary bremsstrahlung in the Born approximation, curve 5 corresponds to the ordinary bremsstrahlung, and the dots stand for the results of Pratt et al.[33]

$|G(\omega,q)|^2$ calculated in these two approximations is retained for other values of the energy ω in the spectral range examined here.

Numerical analysis has shown that practically all the information about multielectron correlations near the $4d$-subshell ionization potential of the La atom is contained in the first factor in (5), while the second depends on correlation effects only weakly.

Figure 5 depicts the dependence of the polarization bremsstrahlung cross section obtained in different approximations for an electron energy of 500 eV. Curve 1 represents the polarization bremsstrahlung spectrum calculated by employing Eq. (6) and using (7) for finding the generalized polarizability. The dipole polarizability $\alpha(\omega)$ is obtained by GRPAE, and the function $G(\omega,q)$ by the Hartree–Fock approximation. The dashed curve $1'$ corresponds to the "exact" Born case within GRPAE, i.e., when both $\alpha(\omega)$ and $G(\omega,q)$ are calculated in GRPAE. The good agreement between the two curves is evident. This shows that the proposed method works well in the range of frequencies $\omega \sim I_{4d}$, i.e., near the peak in the bremsstrahlung spectrum.

Curve 2 in Fig. 5 represents the bremsstrahlung cross section calculated within the above scheme with the dynamic polarizability $\alpha^{exact}(\omega)$ obtained from the experimental data on photoabsorption[24,29] and with the function G^{HF} calculated in the Hartree–Fock approximation.

The discrepancy between the curves 2 and 1 in Fig. 5 can be explained by the difference in the dipole polarizations α^{exact} and $\alpha^{GRPAE}(\omega)$ related to the fact that correlations are fully taken into account in $\alpha^{exact}(\omega)$. This discrepancy is significantly greater than the error introduced by the approximation (7) and is the one that must be accounted for.

Curve 3 in Fig. 5 represents the experimental bremsstrahlung spectrum of 500-eV electrons for metallic La (see Ref. 31). Since the experimental data had no absolute calibration, we normalized the spectral intensity to the peak value of the theoretical cross section. To isolate the polarization component in the experimental spectrum we subtracted the spectrum of ordinary bremsstrahlung determined by in-
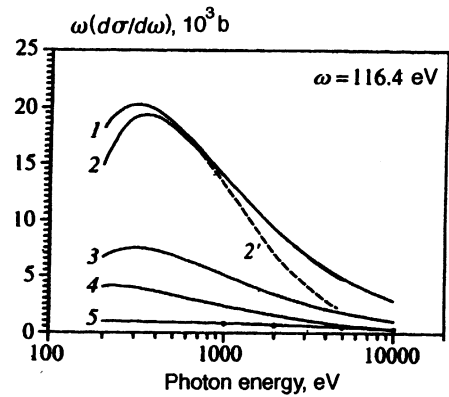
terpolating the results below the resonance and far above it. In addition to the polarization component, this spectrum contains the interference of ordinary and polarization bremsstrahlung, but near the peak the interference is not too essential.

The good agreement between the theoretical cross section obtained by the semiempirical method and the experimental spectrum is evident. A slight difference (about 0.5 eV) in the position of the peaks and a more extended right wing in the experimental spectrum can be attributed to the interference effect, not considered in our model. A method allowing for the interference term within the suggested model is described in Ref. 32.

The Born approximation (4) also contributes to errors, which, however, diminish as the incident-electron energy rises.

The above statement is illustrated by the curves 1 and 2 in Fig. 4, where we have depicted the peak value $\omega(d\sigma/d\omega)_{max}^{pol}$ (i.e., at ω_{max}) as a function of the incident-electron energy, obtained in GRPAE. The Born approximation (curve 1) somewhat overestimates the polarization bremsstrahlung cross section calculated at small values of ε_1 but practically coincides with the curve 2 for $\varepsilon_1 > 1$ keV.

The dashed curve $2'$ depicts the sum of the first 31 polarization bremsstrahlung partial cross sections. As the incident-electron energy is increased, the number of the terms in (3) effectively contributing to the total cross section grows linearly and can be estimated at $l_{eff}^{pol} \sim 2\varepsilon_1/\omega$. On the other hand, the radial wave functions of the incident particle with orbital angular momenta $l \gg v_1 R_{at}$ are distorted only slightly by the atomic field and free-particle wave functions:

$$P_{l,p}(r) = r\sqrt{p/\pi}j_l(pr), \tag{10}$$

where $j_l(pr)$ is a spherical Bessel function.

In this case the bremsstrahlung partial cross sections can be obtained in a closed analytical form, which makes it possible to sum the remainder of the series (3) (see Ref. 23).

Figure 6 shows that starting at $\varepsilon_1 = 500$ eV, the 31 terms in (3) are not sufficient for a meaningful description of the polarization bremsstrahlung cross section.

Curve 3 in Fig. 6 depicts the dependence of the polarization bremsstrahlung cross section in the Born approximation calculated by (7).

Figure 6 also illustrates the dependence of the ordinary bremsstrahlung cross section $\omega(d\sigma/\delta\omega)^{\mathrm{ord}}$ on the energy ε at $\omega = \omega_{\max}$.

Curve 4 in Fig. 6 corresponds to the ordinary bremsstrahlung cross section calculated in the Born approximation, and curve 5 corresponds to the same quantity calculated in the partial-wave approximation. For comparison we also give the data of Ref. 33 (the dots). Comparing curves 4 and 5, we see that the Born approximation considerably overestimates the ordinary bremsstrahlung cross section (see also Ref. 34) for incident-electron energies up to 5 keV.
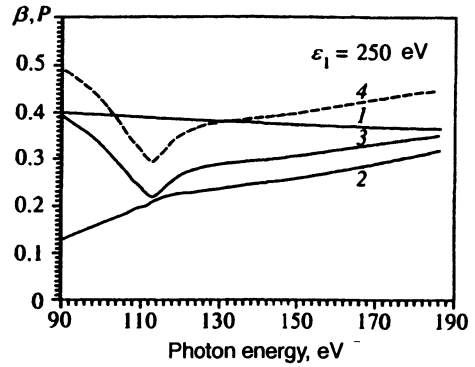

FIG. 7. The angular anisotropy parameter β and the degree of polarization $P(\omega, \pi/2)$ as functions of the photon energy (the partial-wave formalism): curve 1 corresponds to ordinary bremsstrahlung, curve 2 corresponds to polarization bremsstrahlung, curve 3 corresponds to total bremsstrahlung, and curve 4 corresponds to the degree of polarization ($\theta = \pi/2$). The electron energy is 250 eV.

4. ANGULAR DISTRIBUTION AND POLARIZATION OF BREMSSTRAHLUNG

An important characteristic of the bremsstrahlung spectrum is the angular distribution of the emitted radiation. In this case the spectrum is described by the double-differential cross section $\omega(d^2\sigma/d\omega d\Omega_\gamma)$ for emission into the solid angle $d\Omega_\gamma$ in the frequency interval from ω to $\omega + d\omega$.

The double-differential bremsstrahlung cross section has a fairly simple structure in the dipole approximation:

$$\omega\frac{d^2\sigma}{d\omega d\Omega_\gamma} = \frac{1}{4\pi}\omega\frac{d\sigma}{d\omega}[1 - \beta(\omega)P_2(\cos\theta)], \qquad (11)$$

where $\beta(\omega)$ is the angular anisotropy coefficient, $P_2(\cos\theta)$ is a Legendre polynomial, and θ is the angle between the directions of propagation of the incident electron $\mathbf{p}_1$ and the emitted photon $\mathbf{k}$.

The double-differential bremsstrahlung cross section can be decomposed into two components, corresponding to the emission of photons polarized parallel to ($\|$) and perpendicular to ($\perp$) the plane formed by the vectors $\mathbf{p}_1$ and $\mathbf{k}$ (see Refs. 23, 25, and 35):

$$\omega\frac{d^2\sigma}{d\omega d\Omega_\gamma} = \omega\left(\frac{d^2\sigma}{d\omega d\Omega_\gamma}\right)^\| + \omega\left(\frac{d^2\sigma}{d\omega d\Omega_\gamma}\right)^\perp. \qquad (12)$$

Here

$$\omega\left(\frac{d^2\sigma}{d\omega d\Omega_\gamma}\right)^\| = \frac{1}{8\pi}\omega\frac{d\sigma}{d\omega}\{1 - \beta(\omega)[2P_2(\cos\theta) - 1]\},$$

$$\omega\left(\frac{d^2\sigma}{d\omega d\Omega_\gamma}\right)^\perp = \frac{1}{8\pi}\omega\frac{d\sigma}{d\omega}[1 - \beta(\omega)]. \qquad (13)$$

The degree of bremsstrahlung polarization, $P(\omega, \theta)$ can be expression in terms of the angular anisotropy coefficient as

$$P(\omega,\theta) \equiv \frac{\omega(d^2\sigma/d\omega d\Omega_\gamma)^\| - \omega(d^2\sigma/d\omega d\Omega_\gamma)^\perp}{\omega(d^2\sigma/d\omega d\Omega_\gamma)^\| + \omega(d^2\sigma/d\omega d\Omega_\gamma)^\perp}$$

$$= \beta(\omega)\frac{1 - P_2(\cos\theta)}{1 - \beta(\omega)P_2(\cos\theta)}. \qquad (14)$$

The parameter $P(\omega, \theta)$ considered as a function of θ attains its maximum at $\theta = \frac{1}{2}\pi$:

$$P\left(\omega, \frac{\pi}{2}\right) = \frac{3\beta(\omega)}{2 + \beta(\omega)}. \qquad (15)$$

An expression for the angular anisotropy coefficient $\beta(\omega)$, which determines the angular distribution and the degree of bremsstrahlung polarization in the partial-wave approximation, is given in Ref. 23.

Curves 1, 2, and 3 in Fig. 7 illustrate the dependence of the angular anisotropy coefficients for ordinary ($\beta_{\mathrm{PW}}^{\mathrm{ord}}$), atomic ($\beta_{\mathrm{PW}}^{\mathrm{pol}}$), and total ($\beta_{\mathrm{PW}}$) bremsstrahlung on the photon energy near the $4d$-subshell ionization potential. The incident-electron energy ε_1 is 250 eV.

Figure 7 shows that within the stated frequency range, $\beta_{\mathrm{PW}}^{\mathrm{ord}}$ is substantially larger than $\beta_{\mathrm{PW}}^{\mathrm{pol}}$, with both functions exhibiting no singularities near the peak in the polarization bremsstrahlung spectrum. The angular anisotropy coefficient for the total bremsstrahlung cross section behaves differently, however.

For photon energies close to the ionization potential, i.e., where the bremsstrahlung spectrum is determined almost entirely by the polarization component, β_{PW} tends to $\beta_{\mathrm{PW}}^{\mathrm{pol}}$. But for photon energies below the threshold and far above it, i.e., where polarization bremsstrahlung is low, β_{PW} tends to $\beta_{\mathrm{PW}}^{\mathrm{ord}}$.

Thus, the frequency dependence of the angular anisotropy coefficient of total bremsstrahlung experiences a dip near the $4d$-subshell ionization potential.

The dashed curve 4 in Fig. 7 illustrates the frequency dependence of the degree of polarization of bremsstrahlung in the direction perpendicular to that of the incident electron, $P(\omega, \pi/2)$. As with β_{PW}, the degree of polarization experiences strong variations at frequencies close to the maximum in polarization bremsstrahlung.

The solid curves 1, 2, and 3 in Fig. 8 illustrate the dependence of $\beta_{\mathrm{PW}}^{\mathrm{ord}}$, $\beta_{\mathrm{PW}}^{\mathrm{pol}}$, and β_{PW} on the incident-electron
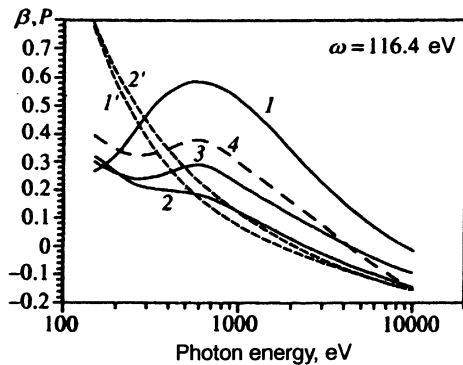
FIG. 8. The angular anisotropy parameter β and the degree of polarization $P(\omega, \pi/2)$ as functions of the incident-electron energy (the partial-wave formalism): curve 1 corresponds to ordinary bremsstrahlung (curve $1'$ represents the Born approximation), curve 2 corresponds to polarization bremsstrahlung (curve $2'$ represents the Born approximation), curve 3 corresponds to total bremsstrahlung, and curve 4 corresponds to the degree of polarization ($\theta = \pi/2$). The photon energy is $\omega = \omega_{max}^{GRPAE} = 116.4$ eV.

energy calculated in the partial-wave approximation. The photon energy corresponds to the peak in the total bremsstrahlung spectrum, $\omega = \omega_{max}^{GRPAE} = 116.4$ eV.

The dashed curves $1'$ and $2'$ illustrate the dependence of the same quantities calculated in the Born approximation.[25] One must bear in mind, however, that the expression obtained in Ref. 25 is valid only for $\omega \ll \varepsilon_1$.

The difference between the results obtained in the partial-wave formalism and in the Born approximation is quite evident in the entire range of electron energies considered here. In the Born approximation the angular anisotropy coefficient monotonically decreases as ε_1 grows, with β_B^{ord} differing little from β_B^{pol}, but the difference is considerable in the partial-wave approximation. The quantity β_{PW}^{ord} has a peak near $\varepsilon_1 = 600$ eV, which is retained in β_{PW}. Similar oscillations of the angular anisotropy coefficient for ordinary bremsstrahlung as a function of the incident-electron energy were discovered by Kim and Pratt,[36] who used the classical-theory approach. They explained the appearance of oscillations in β^{ord} by the superposition of the intensities corresponding to different impact parameters in the scattering of the electron by a screened Coulomb potential.

The dependence of the angular anisotropy coefficient β_{PW}^{pol} is smoother and is in better agreement with that of β_B^{pol}.

The dashed curve 4 in Fig. 8 illustrates the dependence of the degree of polarization of bremsstrahlung $P(\omega_{max}, \pi/2)$ on the incident-electron energy.

5. CONCLUSION

Our calculations of the spectrum of bremsstrahlung from collisions of intermediate-energy and a La atom show that in the vicinity of the $4d$-subshell ionization potential almost all bremsstrahlung is formed by the polarization mechanism.

At photon frequencies $\omega \gg I_{4d}$ the total bremsstrahlung cross section is considerably larger that the ordinary bremsstrahlung cross section at low incident-electron energies ε_1. The effect is caused by interference between ordinary

and polarization bremsstrahlung. As the incident-electron energy grows, the role of interference diminishes.

We have suggested a simple semiempirical method that allows for effects associated with multielectron correlations. A similar method can used to provide a theoretical description of polarization bremsstrahlung involving more complex objects, such as molecules, clusters, and solids.

[1] V. B. Berestetskiĭ, E. M. Lifshitz, and L. P. Pitaevskiĭ, Quantum Electrodynamics, 3rd ed., Pergamon Press, Oxford (1991).

[2] M. Ya. Amus'ya, V. M. Buĭmistrov, B. A. Zon et al., Polarization Bremsstrahlung from Particles and Atoms, Nauka, Moscow (1987) [in Russian].

[3] M. Ya. Amus'ya, A. S. Baltenkov, V. B. Gilerson, Pis'ma Zh. Tekh. Fiz. 3, 1105 (1977) [Sov. Tech. Phys. Lett. 3, 455 (1977)].

[4] É. T. Verkhovtseva, E. V. Gnatchenko, B. A. Zon, A. A. Nakipelov, and A. A. Tkachenko, Zh. Éksp. Teor. Fiz. 98, 797 (1990) [Sov. Phys. JETP 71, 443 (1990)].

[5] T. M. Zimkina, A. S. Shulakov, and A. P. Braĭto, Fiz. Tverd. Tela (Leningrad) 23, 2006 (1981) [Sov. Phys. Solid State 23, 1171 (1981)].

[6] T. M. Zimkina, A. S. Shulakov, A. P. Braĭto et al., Fiz. Tverd. Tela (Leningrad) 26, 1981 (1984).

[7] M. Ya. Amus'ya, T. M. Zimkina, and M. Yu. Kuchiev, Zh. Tekh. Fiz. 52, 1424 (1982).

[8] N. B. Avdonina, M. Ya. Amus'ya, M. Yu. Kuchiev, and L. V. Chernysheva, Zh. Tekh. Fiz. 56, 246 (1986) [Sov. Phys. Tech. Phys. 31, 150 (1986)].

[9] M. Ya. Amus'ya, L. V. Chernysheva, and A. V. Korol, J. Phys. B 23, 2889 (1990).

[10] A. V. Korol, A. G. Lyalin, A. S. Shulakov, and A. V. Solov'yov, J. Phys. B 28, L155 (1995).

[11] M. Ya. Amus'ya, M. Yu. Kuchiev, and A. V. Solov'ev, Zh. Éksp. Teor. Fiz. 89, 1512 (1985) [Sov. Phys. JETP 62, 876 (1985)].

[12] M. Ya. Amus'ya, M. Yu. Kuchiev, and A. V. Solov'ev, Pis'ma Zh. Tekh. Fiz. 11, 1401 (1985) [Sov. Phys. Tech. Phys. Lett. 11, 577 (1985)].

[13] K. Ishii and S. Morita, Phys. Rev. A 31, 1168 (1985).

[14] A. V. Solov'ev, Z. Phys. D 24, 513 (1992).

[15] M. Ya. Amus'ya, The Atomic Photoelectric Effect, Nauka, Moscow (1987) [in Russian].

[16] M. Ya. Amus'ya, V. K. Ivanov, S. A. Sheĭnerman, and S. I. Sheftel', Zh. Éksp. Teor. Fiz. 78, 910 (1980) [Sov. Phys. JETP 51, 458 (1980)].

[17] G. Wendin, Phys. Lett. A 51, 291 (1975).

[18] M. Ya. Amusia, V. K. Ivanov, and L. V. Chernysheva, Phys. Lett. A 59, 191 (1976).

[19] M. Ya. Amusia and N. Cherepkov, Case Studies in Atomic Physics 5, 47 (1975).

[20] M. Ya. Amus'ya, Bremsstrahlung, Energoatomizdat, Moscow (1990).

[21] M. Ya. Amusia and A. V. Korol, J. Phys. B 24, 3251 (1991).

[22] L. V. Chernysheva, N. B. Avdonina, M. Ya. Amus'ya, and A. V. Korol', Preprint 1314, A. F. Ioffe Physicotechnical Institute, Leningrad (1989).

[23] M. Ya. Amusia and A. V. Korol, J. Phys. B 25, 2383 (1992).

[24] M. Richter, M. Meyer, M. Pahler et al., Phys. Rev. A 39, 5666 (1989).

[25] M. Ya. Amusia, N. B. Avdonina, L. V. Chernysheva, and M. Yu. Kuchiev, J. Phys. B 18, L791 (1985).

[26] A. V. Korol. J. Phys. B 25, L341 (1992).

[27] B. A. Zon, Zh. Éksp. Teor. Fiz. 77, 44 (1979) [Sov. Phys. JETP 50, 21 (1979)].

[28] A. V. Korol, A. G. Lyalin, and A. V. Solov'yov, Phys. Rev. A 53 (1996) (in press).

[29] T. M. Zimkina and S. A. Gribovskii, J. de Phys. Coll. C-4, Sup. 10, 32, C4-282 (1971).

[30] B. L. Henke, E. M. Gullikson, and J. C. Davis, At. Data Nucl. Data Tables 54, 2 (1993).

[31] T. M. Zimkina, A. S. Shulakov, and A. P. Braĭko, Izv. Akad. Nauk SSSR, Ser. Fiz. **48**, 1263 (1984).

[32] A. V. Korol, A. G. Lyalin, and A. V. Solov'yov, J. Phys. B **29** (1996) (in press).

[33] R. H. Pratt, H. K. Tseng, C. M. Lee et al., At. Data Nucl. Data Tables **20**, 175 (1977).

[34] B. A. Zon, Zh. Éksp. Teor. Fiz. **107**, 1176 (1995) [JETP **80**, 655 (1995)].

[35] N. B. Avdonina, M. Ya. Amus'ya, M. Yu. Kuchiev, and L. V. Chernysheva, Izv. Akad. Nauk SSSR, Ser. Fiz. **50**, 1261 (1986).

[36] L. Kim and R. H. Pratt, Phys. Rev. A **36**, 45 (1987).

[37] M. Ya. Amus'ya and L. V. Chernysheva, An Automatic System for Atomic Structure Studies, Nauka, Leningrad (1983) [in Russia].

Translated by Eugene Yankovsky